Uncovering Individualized Cerebellar Atrophy Pattern and Behavioral Links in Children with Brainstem Tumor

Heyuan Jia,[1,2,†] Kaikai Wang,[3,†] Mingxin Zhang[4], Guocan Gu[4], Yiying Mai[4], Xia Wu[3], Congying Chu[3], Xuntao Yin[5], Peng Zhang[4], Lingzhong Fan[3,6] and Liwei Zhang[4,7,8]

[†]These authors contributed equally to this work.

Author affiliations:

1 School of Instrumentation and Optoelectronic Engineering, Beihang University, Beijing, China

2 Institute of Large-scale Scientific Facility and Centre for Zero Magnetic Field Science, Beihang University

3 Brainnetome Center, Institute of Automation, Chinese Academy of Sciences, Beijing 100190, China

4 Department of Neurosurgery, Beijing Tiantan Hospital, Capital Medical University, Beijing, China

5 Department of Radiology, Guangzhou Women and Children's Medical Center, Guangzhou Medical University, Guangzhou, China.

6 School of Health and Life Sciences, University of Health and Rehabilitation Sciences, Qingdao 266000, China.

7 China National Clinical Research Center for Neurological Diseases, Beijing Tiantan Hospital, Capital Medical University, Beijing, China

8 Beijing Neurosurgical Institute, Beijing Tiantan Hospital, Capital Medical University, Beijing 100070, China.

Correspondence to: Liwei Zhang, Professor

Department of Neurosurgery, Beijing Tiantan Hospital, Capital Medical University, Beijing, China

E-mail: zhangliweittyy@163.com

Lingzhong fan, Professor

Brainnetome Center, Institute of Automation, Chinese Academy of Sciences, Beijing 100190, China

E-mail: lingzhong.fan@ia.ac.cn

Zhang Peng, M.D.

Department of Neurosurgery, Beijing Tiantan Hospital, Capital Medical University, Beijing, China

E-mail: zhang_roc@163.com

Abstract

Background

Brainstem tumors are rare and result in enduring behavioral issues, posing challenges for patients and surgeons. Despite similarities in symptoms to those resulting from cerebellar injuries, limited research has investigated cerebellar changes in patients with brainstem tumors.

Methods

Here, we employed U-Net-based segmentation to analyze the cerebellum in 26 regions, assessing individual volume deviations. Additionally, we developed a behavior prediction model using the total outlier count (tOC) index and brain volume as features.

Findings

Our normative model results revealed that most patients exhibited negative deviation in most cerebellar regions, particularly in lobule Right V, Left I-III, Right X, and Left X. The results found a significant association between a higher tOC and severe social problems ($r = 0.31$, $p = 0.001$) and withdrawal behavior ($r = 0.28$, $p = 0.001$). Further analysis showed that smaller cerebellar regions correlated strongly with more pronounced social problems ($r = 0.27$, $p = 0.007$) and withdrawal behavior ($r = 0.25$, $p = 0.015$). Notably, lobules such as Right X, V, IV, and VIIB, along with Left IX, VIII, and X exerted the greatest influence on social problems, whereas regions including Left V, Right IV, and Vermis VI and VIII were most impactful on withdrawal behavior.

Interpretation

In summary, our study revealed cerebellar atrophy patterns in patients with brainstem tumors, emphasizing the role of both anterior and posterior cerebellar lobes in social problems and withdrawal behavior. This research sheds light on the brain mechanisms underlying complex behavioral disorders in brainstem tumor patients.

Funding

This study was supported by the STI2030-Major Projects 2021ZD0200201 and Beijing Municipal Public Welfare Development and Reform Pilot Project for Medical Research Institutes (grant ID: JYY202X-X).

Keywords: Brainstem tumor; cerebellar atrophy; social problem; normative model; machine learning

Research in Context

Our previous neuropsychological research has demonstrated that patients with brainstem tumors exhibit a wide range of cognitive and behavioral abnormalities, which closely resemble cerebellar cognitive affective syndrome (CCAS). Dines et al. hypothesized, based on cognitive impairment observed in patients with brainstem injury, that the brainstem, as an integral part of the cerebellar-cortex pathway, plays a role in cognitive processing. Consequently, brainstem injury may lead to cerebellar dysfunction. Previous studies have also reported that gangliocytoma located in the brainstem can cause ipsilateral cerebellar atrophy. These findings suggest that cerebellar injury may be present in patients with brainstem tumors. However, no systematic studies have investigated the pattern of cerebellar injury in these patients and its association with cognitive and behavioral disorders.

Added value of this study

This study revealed the pattern of cerebellar heterogeneity in patients with brainstem tumors. Further, this study provides evidences for the cerebellum's role beyond motor control, underscoring its involvement in complex social behaviors. This study provides insight into automatic cerebellar segmentation algorithm applied to patients’ dataset.

Implications of all the available evidence

This study is first to successfully apply machine learning for segmenting deformed cerebellums, providing a reference for future large-sample studies of diseased cerebellum and brainstems. Moreover, this study provides evidence that the brainstem and cerebellum are involved in complex cognitive processing. Future research should focus on developing personalized treatment and rehabilitation programs for patients with brainstem tumors and cerebellar injury to improve their prognosis.

.

Introduction

Brainstem tumors originate specifically in the medulla oblongata, pons, and midbrain(1). They constitute 15% of pediatric brain tumors, with diffuse intrinsic pontine gliomas (DIPG) making up 80% of these cases(2). Unfortunately, DIPG in children is associated with a very poor prognosis and leads to complex neurological dysfunction. Previously, researchers did not attribute higher cognitive processes to the brainstem(3). However, an increasing number of neurosurgeons report abnormal cognitive and behavioral disorders in patients with brainstem lesions. These broad behavioral deficits are often masked by a patient's personality or complex neurological symptoms(4). Notably, atypical symptoms, such as behavioral disorders(5, 6), withdrawal(7), attention deficits(8), social disturbances(9), irritability(10, 11), and flattened affect(5), are gaining increased attention in clinical assessment. In some cases, these symptoms persist for over half a year after surgical intervention(12, 13). Recent neuropsychological research has also demonstrated widespread behavioral impairments in children with brainstem occupying(14).

Current research suggests the involvement of the brainstem in cognitive processing through various mechanisms. Specifically, researchers hypothesize that the brainstem, as a distant brain region, interacts with the frontal lobe system, influencing cognitive function(4). Recent functional connectivity studies indicate that multiple organizational features of cortical activity can be traced back to the brainstem(15). One perspective suggests the involvement of the pons in cognitive processing, with the cerebellum as an integral component of the cerebello-cerebral circuit(16). Clinical observations support this hypothesis. In light of the frequent co-occurrence of cerebellar damage in posterior fossa tumors, brainstem tumors often present symptoms resembling cerebellar injuries, particularly ataxia, and typically indicate an unfavorable outcome(4). Clinicians frequently observe concurrent cerebellar changes in patients with brainstem injuries. Ipsilateral cerebellar atrophy is common in brainstem tumor cases(17), as well as in cases of brainstem ischemia, stroke, and trauma(18, 19), possibly due to the proximity and extensive direct fiber connections between the brainstem and cerebellum(20-23). The corticospinal tract and spinocerebellar tract are the primary neural pathways that connect cortical brain regions with the contralateral cerebellum through the intermediary pontine region(24). Simultaneously, fascicular pontocerebellar fibers traverse the midline, radiating extensively into the opposite hemisphere before converging within the contralateral cerebellum(25, 26). These connections form three pairs of

cerebellar peduncles, which are crucial for cerebellar function(27). Moreover, the cerebellum establishes connections with various brain regions, including the hypothalamus, limbic system, and brainstem regions such as the ventral tegmental area, periaqueductal gray matter, and locus coeruleus(28).

While brainstem injury can lead to varying degrees of cerebellar damage, there has been limited systematic investigation into the indirect cerebellar changes and their relationship with cognitive functions in patients. The highly specialized internal functional mapping of the cerebellum relies on its complex anatomical structure and connections(29). Functional imaging studies have demonstrated that various cognitive tasks can activate specific cerebellar regions, exhibiting distinct topographic distribution characteristics. These tasks include multiple cognitive and affective processing representations, primarily localized in three focal regions: lobule VI to Crus I, Crus II to VIIB, and lobule IX to lobule X(30, 31). For example, language tasks activate the right lateral cerebellum, while visuospatial tasks engage lobules VI and Crus I. Working memory tasks activate bilateral posterior cerebellar regions, and affective processing tasks engage lobules VI and VII(32, 33). In summary, anterior cerebellar lobules I-IV and lobule VIII are primarily linked to motor functions, whereas posterior and lateral cerebellar lobules are associated with non-motor functions(34). Schmahmann consolidated various indicators such as executive, visuospatial, linguistic, and affective deficiencies, resulting from lesions in the posterior cerebellar lobes, terming it the cerebellar cognitive affective syndrome (CCAS)(35). This amalgamation of cognitive and neuropsychiatric challenges consistently emerges in subsequent investigations of cerebellar diseases across adult and pediatric populations, subject to rigorous scrutiny(36, 37). Moreover, cognitive and behavioral impairments caused by brainstem tumors closely resemble the CCAS(16). Hence, we hypothesized that damage to the cerebellar cortex resulting from brainstem lesions exhibits significant heterogeneity, contributing to a range of behavioral, cognitive, and emotional impairments in patients.

To test our hypothesis and explore patterns of cerebellar injury caused by brainstem tumors, we employed the ACAPULCO (Automatic Cerebellum Anatomical Parcellation using U-Net with Locally Constrained Optimization) for cerebellar segmentation in our patients. Additionally, we employed a normative model, a statistical tool commonly used to establish quantitative relationships between variables and brain features. This approach, different from traditional case-control analyses, accommodates the clinical and biological heterogeneity present in our study group. Moreover, we integrated phenotypic data from healthy children to

construct a normative model, allowing us to quantify individual deviations in our brainstem tumor patients. Lastly, to establish a link between these deviations and corresponding behaviors, we used machine learning techniques.

Patients and methods

Participants

We enrolled a cohort of 171 pediatric patients diagnosed with brainstem tumors at the Department of Neurosurgery, Beijing Tiantan Hospital, between April 2019 and December 2022. Inclusion criteria were as follows: 1) Initial diagnosis of brainstem tumor with no prior treatment; 2) Tumors confined to the brainstem without infiltrating the cerebellum, spinal cord, or thalamus; 3) Absence of comorbid psycho-neurological disorders, behavioral and personality disorders; 4) No history of developmental disorders. All patients underwent 3DT1 magnetic resonance imaging (MRI) during their initial visit and completed the Child Behavior Checklist (CBCL) scale - Parent version. Informed consent was provided by the parents of all participants as per the Institutional Review Board-approved protocol obtained from the Beijing Tiantan Hospital, Capital Medical University.

To establish a normative model, we collected data from healthy children through publicly ava ilable databases, primarily from four distinct sources. The first source comprised 61 healthy c hildren locally recruited in Beijing. The second source included 69 children from the fcon_10 00. projects dataset (http://fcon_1000.projects.nitrc.org/indi/CoRR/html/samples.html). The t hird source contained data from the Child Connectome Project (CCNP), including 450 childr en (developing Chinese Color Nest Project (devCCNP) Lite (scidb.cn))(38). Data from the fo urth source were obtained from the Children’s Hospital in Guangzhou, involving 269 childre n. We downloaded MRI T1 images and corresponding phenotypic information from these dat abases, with the demographic characteristics of the subjects summarized in Table 1.

After excluding subjects with severe cerebellar compression and those with poor image scann ing quality, our final analysis included 147 patients and 849 healthy children. Supplementary Fig. 1 illustrates the enrollment process in a flowchart.

Table 1. The demographic of cohort and clinical characteristic

Variables	Patients/N (%)	Healthy Children/N (%)
Data site		
Beijing Tiantan Hospital	147	61
IPCAS		69
CNNP		450
Guangzhou Children's Hospital		269
Total	147	849
Sex		
Male	77(55.5%)	477(53.9%)
Female	70(44.5%)	372(46.1%)
Age (Mean, SD, min-max)/years	8.5(3.5), (4-17)	11.44(3.3), (4-18)
Tumor location		
Pontine	114(77.6%)	
Midbrain	15(10.2%)	
Medulla	18(12.2%)	

MRI acquisition and processing

MRI DATA acquisition

A structural MRI scan was performed for all participants using a 3.0 T scanner (Ingenia CX, Philips Healthcare, Best, the Netherlands) equipped with a 32-channel head receiver coil. The scan comprised a whole-brain 3D T1-weighted (3DT1) anatomical sequence consisting of 196 contiguous sagittal slices with a voxel size of 1.0 x 1.0 x 1.0 mm3. The specific parameters of 3D-T1 were as follows: repetition time (TR) =6.572ms; echo time (TE) =3.025 ms; flip angle (FA) = 8°; slice thickness = 1mm; in-plane resolution = 1*1mm. The typical radiological characteristics are presented in Fig. 1.

Data Processing

The original DICOM images were converted to NIFTI format. Due to tumor-related deformation, varying degrees of distortions were observed in the cerebellar of patients. To ensure accurate segmentation and avoid misclassifying the brainstem as the cerebellum, researchers with expertise in neurosurgery delineated the brainstem as the volume of interest (VOI) in advance. VOI delineation was performed using MRIcroGL and the "Delete regions with VOI" tool. After preprocessing, automatic segmentation of cerebellar lobules in all participants was achieved using ACAPULCO software (version 0.2.1)(39), coupled with a

pediatric template(40). Image inhomogeneities were corrected using N4 correction(41). The corrected image was rigidly registered to MNI space using the 1 mm isotropic ICBM 2009c template(42). A bounding box enclosing the cerebellum was delineated, and a modified U-Net architecture was used for individual lobule segmentation. The segmented image was transformed back to its original image space, enabling the calculation of volumes for each region of interest (ROI).

To ensure segmentation accuracy, the cerebellar parcellations underwent visual inspection by two independent researchers. Any discrepancies observed were resolved through consensus discussions. Over-segmented non-cerebellar areas and under-segmented cerebellar regions were manually corrected using ITK-SNAP(43). Ultimately, volumes were obtained for 28 distinct cerebellar regions, including both left and right lobules I-III, IV, V, VI, VIIB, VIIIA, VIIIB, IX, X, Crus I, Crus II, as well as vermis lobules VI, VII, VIII, IX, X, and corpus medullare. To account for the non-uniform margin between lobules VIIIA and VIIIB, they were combined into a single lobule, designated as lobule VIII. Consequently, 26 independent cerebellar region volumes were used for analyzing individualized cerebellar changes and their associations with behavioral outcomes.

Behavioral assessment

Participants' behavioral profiles were assessed using the Achenbach Child Behavioral Checklist (CBCL), designed for individuals aged 4-18. The questionnaire comprises 113 items, categorizing behavioral issues into eight factors: somatic symptoms, withdrawal, depression/anxiety, aggressive behavior, delinquent behavior, thought problems, and social problems. The first three factors fall under internalized problems, while aggressive and delinquent behavior are considered externalized problems(44).

Data harmonization

We utilized the Combat method to harmonize data from three distinct datasets, thereby thereby mitigating non-biological variance arising from inter-scanner discrepancies(45). The Combat method has been validated for effectively reducing unwanted variation introduced by site differences in structure MRI investigations or DTI(46, 47), while preserving biological

variability. Specifically, we applied the Combat method to harmonize data from individual sites to ensure consistency across all datasets. Notably, we retained age, gender, and TIV as covariates while excluding diagnostic labels.

Normative modeling

After obtaining volumetric data for the 26 cerebellar regions from all participants, we established normative models using Python version 3.9 and PCNToolkit version 0.22 (https://github.com/amarquand/PCNtoolkit). We employed the Gaussian Process Regression (GPR) model, trained on the dataset of healthy individuals, to generate region-specific normative models, incorporating age and gender as covariates(48). The Gaussian Process Regression (GPR) technique, implemented within the PCNToolkit, accommodated gender and age as covariates to predict region volumes. This Bayesian non-parametric modeling approach inherently considers prediction uncertainty and provides probability distributions for predicted values. To evaluate the robustness of these models, we initially estimated normative models across the entire healthy control (HC) dataset using a 10-fold cross-validation strategy. Subsequently, definitive normative models were developed based on the entire healthy cohort for subsequent deviation analyses in patients. For each participant, the normative model was used to predict volume estimates for each region, along with corresponding predictive uncertainty. Predictive uncertainty contours were then used to characterize centile variations within the cohort, enabling us to parameterize volume deviations relative to the reference cohort.

Estimation of cerebellar volume deviations for each subject

For each glioma patient, we utilized normative percentile charts established from healthy control to assess individual deviations in cerebellar region volumes. To quantify these deviations from the normative model for each region, we computed a Z score based on observed and predicted volume values obtained from the model. For each patient i, the Z score of a cerebellum region j was calculated using the formula:

$$Z_{ij} = \frac{y_{ij} - \hat{y}_{ij}}{\sqrt{\sigma_{ij}^2 + \sigma_{nj}^2}} \qquad (1)$$

where y_{ij} is the true volume value, $\hat{y}_{ij}$ *is* the expected volume value estimated from the GPR, σ_{ij} is the predictive uncertainty, and σ_{nj} is the variance learned from the normative distribution n.

Statistical Analysis

Deviation rate calculation and statistics

Using the normative model, we can evaluate the relative deviation distribution for each patient compared to the general norm. While moderate deviations are expected due to individual variability, detecting significant shifts across all brain regions in individuals is clinically significant. We compute the deviation rate to quantify the degree of deviation in each brain region. This involves dividing the count of patients with Z values exceeding 1.96 by the total patient count (positive deviation rate) and using a similar approach for Z-values less than -1.96 (negative deviation rate).

Outlier definition

Outliers indicating diminished cerebellar volume were identified within each region, precisely defined as $Z < -1.96$, corresponding to the lower 2.5th percentile of the normative cerebellar volume distribution. We selected the lower threshold for outlier detection to focus on evaluating reductions in cerebellar volume associated with glioma. The total outlier count (tOC) across all 26 regions was computed for each participant(49).

Outlier associations with social problems and withdrawal

We investigated the relationship between tOC and clinical symptoms, specifically social problems and withdrawal. Pearson correlation analysis was performed to examine the correlation between tOC and these symptoms. Furthermore, we explored whether tOC could serve as an indicator for essential behaviors in pediatric patients diagnosed with a brainstem tumor. To investigate this, we used tOC as a feature to represent the extent of atrophy in individual cerebellar regions. Employing a ridge regression model (https://scikit-learn.org/stable/), we assessed whether tOC could predict correlated behavioral scores. We

implemented a nested fivefold cross-validation (5F-CV) procedure, where an outer loop assessed the model's generalization to unseen subjects, while the inner loop performed a grid search algorithm to identify the optimal parameter within a specified λ range ($[2^{-10}, 2^{-9}, \ldots, 2^{4}, 2^{5}]$(50). Due to the random partitioning of the data into five groups, we conducted 101 repetitions of the 5F-CV procedure. The prediction accuracy of each run in the outer loop was calculated as the mean r value between the five folds. Thus, the final prediction accuracy of the model was determined as the median r value of 101 replicates. Within each cross-validation fold, a linear regression was applied to eliminate age and sex effects from the training data features. The coefficients obtained from the training data were then used to regress these covariates from the testing data features. Permutation testing was employed to assess the significance of the prediction. This method estimated the empirical distribution of prediction accuracy assuming a null hypothesis: no association between the cerebellar volume deviation patterns and behavior values. To create the null distribution, the complete prediction procedure was repeated 1000 times. In each iteration, the behavior scores were permuted across the training samples(50).

Prediction behaviors from cerebellar volume deviations using ridge regression

After analyzing the relationship between tOC and behavior, we investigated whether cerebellar volume deviations captured significant behavioral characteristics in pediatric glioma patients. To address this question, we combined the Z scores from 26 regions into a comprehensive feature vector representing an individual's deviation. Subsequently, we adjusted the ridge regression model using these volume deviations. In each multivariate model, each region was assigned a feature weight, with the weight's magnitude indicating its importance, and its sign revealing a negative or positive association with both cerebellar volume and behaviors. Across 101 iterations, we evaluated the weight of each feature in the run corresponding to the median r value. Through 1000 permutation tests, we determined the significance of each feature weight. A positive weight at a region would imply that the volume of that brain region is greater in individuals with higher behavior scores. Conversely, a negative weight at a region would suggest that the volume of that region is reduced in individuals with higher behavior scores.

Role of funders

Results

Demographics of the cohort and clinical characteristics

Initially, we enrolled 171 pediatric patients diagnosed with brainstem tumors and 849 typically developing children from 8 different sites. After excluding cases with poor MRI scanning (6 patients, 8 healthy children), those with tumors involving the cerebellum or thalamus (6 patients), and those with segmentation issues (10 patients), our final analysis comprised 147 patients, with a mean age of 8.5 years and 77 males. Among these patients, 114 had tumors located in the pontine region, 18 in the medulla oblongata, and 15 in the midbrain. We constructed a normative model using data from 849 typically developing children, with a mean age of 11.44 years old and 477 males (see Table 1). Fig. 2 showed the flow chart of the whole experiment.

Individual deviation of cerebellar volumes in patients

The normative trajectory derived from the GPR model for four cerebellar regions with the most extreme deviation demonstrated that abnormal deviation values in patients primarily fell below the lower boundary (Fig. 3A). The violin chart indicates that the majority of both patients and healthy children exhibited zero extreme positive deviations, with only 2.5% of subjects showing such deviations. Gender distribution showed no significant differences. In contrast, extreme negative deviations in healthy children were minimal and concentrated around zero, whereas in patients, these deviations were more evenly distributed, ranging from 3 to 10 in 95% of cases. Female patients exhibited a higher prevalence of extreme negative deviations compared to males (Fig. 3B). The stacked histogram suggested that patients primarily displayed positive deviations in the corpus medullare, while negative deviations were predominantly observed in Left I-III, Left V, Right V, Right I-III, Right X, Left X, Left IV, Vermis VI, Right IV, Vermis VII, and Right VIII (Fig. 3C).

Outliers are associated with cognitive function

Our findings reveal a significant predictive relationship between the tOC and individuals' behavior scores. Specifically, we observed that the tOC correlated with cognitive function (social problems: r = 0.31, p = 0.001; withdrawn: r = 0.28, p = 0.001, Fig. 4A, 4B). Moreover, the tOC can predict scores related to social problems [Mean r = 0.27, P =0.030] and withdrawal [Mean r = 0.25, P = 0.034] (Fig. 4C, 4D). There exists a positive linear relationship between toc and social problems as well as withdrawal, indicating that higher toc values correspond to more severe social problems and withdrawal.

Predictive relationship between cerebellar volume deviations and behavior in glioma patients

Using the ridge regression model, we discovered a significant predictive association between cerebellar volume deviations and individuals' behavior scores. Specifically, our analysis revealed that cerebellar volume deviations could predict scores associated with social problems (r = 0.27, p=0.007) (Fig. 5A), withdrawn (r = 0.25, p = 0.015) (Fig. 5C).

We observed that the region contribution weights predominantly displayed negative values, indicating reduced cerebellar volume in regions corresponding to more severe symptoms. For example, negative feature weights were evident in regions such as Right X, Right V, Right IV, Left IX, Left VIII, Left X, Left V, and Right VIIB for social problems (Fig. 5B), and in regions like Left V, Right IV, Vermis VIII, Left X, Left IV, Left IX, Vermis VI, Right X, Right VIIB, Vermis X, Right Crus I, and Right V for withdrawal (Fig. 5D). Furthermore, negative feature weights were consistent across both correlated behaviors in regions including Right X, Left X, Right V, Left V, Right IV, and Left IX.

Discussion

This individualized investigation revealed a general reduction in cerebellar gray matter among patients diagnosed with brainstem tumors, demonstrating a heterogeneous pattern of atrophy. Particularly noteworthy were the significant negative deviations observed in Left I-

V, right I-V, and Vermis IV-VII. Additionally, a negative correlation was identified between the degree of cerebellar lobe deviation and withdrawal behavior as well as social problems. Moreover, the comprehensive total outlier score emerged as an individualized indicator of cortical atrophy for subsequent analyses. In summary, the aforementioned findings yield the following insights: 1) Brainstem tumors disrupt the normal neuroanatomical development of the cerebellum. 2) The neural mechanisms underlying certain behavioral issues observed in children with brainstem tumors may be associated with abnormal cerebellar structure. 3) Individual indicators of cerebellar lobular atrophy hold promise as predictors of behavioral outcomes.

Cerebellar atrophy patterns in children with brainstem tumors

Severe atrophy predominantly affects the anterior lobes and vermis cerebelli, with a milder impact on the posterior and lateral lobes. This specific pattern of atrophy likely arises primarily from compression due to the swollen brainstem. The current findings support existing clinical research highlighting the occurrence of secondary cerebellar atrophy induced by brainstem tumors. For example, previous studies have reported significant overall cerebellar atrophy in patients with basal gangliocytoma involving the cerebellar peduncles through subjective diagnosis by neurosurgeons(17, 51). Interestingly, cerebellar atrophy is a common occurrence in patients with brainstem diseases. Recent research has elucidated distinctive patterns of decreased cerebellar grey matter volume in patients with left and right pontine infarctions, emphasizing the importance of considering the lateralization of brain lesions in understanding cerebellar structural alterations(52).

Research indicates that the cerebellum undergoes rapid growth during the trimester(53, 54) and continues to grow with an increase in intra-cerebral cellular processes and white matter proliferation during adolescence(55). The volume of microstructures in the cerebellar peduncles increases until the age of 30(56). Various factors, such as cerebellar hemorrhage, tumors, and indirect damages like diaschisis, can lead to a loss of cerebellar volume. Additionally, studies on traumatic brain injury and animal models have demonstrated instances of cerebellar atrophy, even without direct damage to the cerebellum(57, 58). The mechanism behind cerebellar atrophy can be attributed to three main reasons. Firstly, the compressions of the posterior fossa space by the swollen brainstem may limit the normal

neurodevelopment of the cerebellum in children, resulting in a general reduction in cerebellar gray matter volume in patients. Secondly, cerebellar atrophy may result from disruptions in anatomical pathways. Impairment of the pontocerebellar fibers can lead to axonal transport obstruction between the cerebellum and brainstem, causing damage to the cerebellar tract and subsequent deformation of cerebellar neurons(17). Additionally, disruptions of the middle cerebellar peduncles in patients with brainstem tumors were observed in our previous white matter study(1). Thirdly, interruption of transsynaptic communication between the pontine and cerebellar regions directly impacts the fiber projection from cerebellar relay neurons to the Purkinje cells in the cerebellar cortex, resulting in irreversible functional inactivation and long-term structural changes in the cerebellum(59).

Correlation between individual cerebellar deviation and behavior

Our study represents a pioneering effort to elucidate the link between secondary structural changes in the cerebellum caused by brainstem tumors and the observed behavioral patterns in pediatric patients. We utilized tOC as a quantitative metric to assess the degree of cerebellar atrophy at an individual patient level. tOC has shown high stability and reliability in predicting individualized neuroanatomical heterogeneity among patients with Alzheimer's disease(49). The identified correlation between tOC and behavior highlights that heightened cerebellar atrophy corresponds to increased withdrawal behavior and social problems in children. The prospective use of tOC as a metric for evaluating compromised cerebellar health in individual patients could offer valuable insights to inform clinical decision-making. This discovery reaffirms the pivotal role of the cerebellum in regulating social functions and provides empirical evidence of its significance as a distinct core brain region(60).

Furthermore, our study found that negative deviations in the volume of cerebellar subregions were significantly associated with worse social behaviors. Specifically, the volume of posterior cerebellar regions, such as lobules X, IX, and VIII, exhibited a significant negative correlation with social problems. These findings are consistent with previous studies, reinforcing the idea that the posterior cerebellar lobes contribute to social functions(61). Additionally, certain parts of the anterior cerebellar lobe, particularly lobule IV and V, implicated in the motor network, suggest that cerebellar regions involved in social functions are complex and not confined to a singular cerebellar region. For instance, functional MRI

neuroimaging during social cognitive tasks has revealed activation of posterior cerebellar regions alongside engagement of the somatosensory motor network(60). This intricate relationship underscores the complexity of cerebellar involvement in social functions. Animals with disrupted activity in anterior lobule IV/V exhibited deficits in object recognition and social associative recognition tests, providing further evidence of the multifaceted role of cerebellar regions in cognitive and social processing(62).

In cerebellar research, a longstanding hypothesis posits that social dysfunction primarily originates from damage in the vermis and posterior cerebellum(63). This hypothesis aligns with the dichotomous theory of cerebellar functions, distinguishing between sensorimotor and cognitive-affective regions, based on anatomical connectivity patterns. Specifically, the spinal cord, brainstem (including the lower olivary nucleus and basal pontine neurons), and regions of the cerebral cortex associated with sensorimotor processing exhibit prominent connections with the anterior cerebellar lobe (comprising lobules I-V) and lobule VIII. There is a relatively lesser degree of connectivity extending to lobule VI and the interpositus nucleus (encompassing the globular nucleus and embolic nucleus). Notable targets of these connections include the lower olivary nucleus, responsible for processing non-motor input, and the brain association area located at the base of the cerebellar bridge. This complex neural network includes lobules VI, VII, and the dentate nucleus. Additionally, limbic structures establish connections with the apex nucleus of the vermis(64). However, the latest perspective suggests that the cerebello-thalamo-cortical (CTC) and cerebello-ponto-cortical (CPC) tracts establish connections between the posterior cerebellum, Crus I/II, and the social regions located in the frontal lobe(65, 66). Consequently, researchers hypothesize that any injury along this pathway is likely to manifest as social deficits. Damage to the areas surrounding the origin of the CTC and CPC tracts can predict social and emotional disorders(67).

Moreover, it is important to note that withdrawn behavior represents a distinct social behavior. Both the anterior and posterior cerebellar lobes and the vermis exhibit significant correlations with withdrawn behavior, with the anterior cerebellar lobe contributing the most weight to this association. Considerable evidence supports the idea that social withdrawal arises from dysfunction within the brain's social decision-making network(68). The cerebellum and brainstem primarily contribute to the somatic motor nuclei within the social decision-making network(69). The pathological withdrawal observed in patients may be attributed to severe atrophy of cerebellar motor nuclei. These findings corroborate numerous

clinical observations indicating that children with lesions in the posterior fossa exhibit more complex and severe social problems, including withdrawal, attention deficit, irritability, pathological crying and laughing, and compression(70). Importantly, extensive damage to the brainstem and cerebellar pedunculum results in more pronounced social dysfunction, with these behavioral disorders being profound and enduring(71).

This study is the first to investigate individual cerebellar changes in patients with brainstem tumors using automated segmentation techniques with the U-Net model. Unlike previous studies that relied on basic diameter measurements or subjective assessments, our approach provides precise quantification of cerebellar atrophy, allowing for larger-scale clinical research. By utilizing normative model, our study mitigates clinical and biological heterogeneity, enhancing the robustness of our findings.

A major contribution of our study is establishing a link between cerebellar damage from brainstem tumors and social behavior. While the impact of cerebellar injury on social functioning is known, neuroimaging evidence of cerebellar damage has been limited. Our study shows that damage to cerebellar regions around CPC and CTC tracts directly impairs social functions, expanding the focus beyond the cerebellar vermis. Additionally, the employment of ridge regression provides valuable insights for large-scale neuroimaging studies in clinical practice.

However, the study has some limitations. The normative model included only age and gender, missing factors like education and home environment. The questionnaire may not capture all aspects of social function. Furthermore, our findings are correlative, not causal, necessitating further research using advanced techniques like DTI, fMRI, and MRS to explore cerebellar microstructure and metabolism for a comprehensive understanding of cerebellar alterations and behavioral outcomes(72).

In conclusion, this study found significant individual heterogeneity regarding the impact of brainstem tumors on the cerebellum which is ascribed to variations in their location and pathological characteristics. Despite its prevalence, this aspect is often underemphasized due to the rarity of brainstem tumors. This study presents a quantitative approach for assessing this variability at the individual patient level by analyzing the spatial patterns of deviations in individual cerebellar region-of-interest (ROI) volumes. Individualized profiles of neuroanatomical outliers are associated with behavioral disorders. Notably, the count of outliers and cerebellar lobules' volume profiles contribute to predicting social behavioral

issues due to their individual patterns. These findings expand our understanding of the crucial role played by the intact brainstem and cerebellar circuits in the modulation social behavior. The robust correlation between unresected tumor-induced disruptions in anatomical pathways and cognitive function has contributed significantly to advancing tumor neuroscience research. In addition, functional assessments of patients before surgery is crucial to enhancing the diagnosis, treatment and allows the preservation of neural pathways during surgical interventions.

Contributors

Experimental design: (Lingzhong Fan, Liwei Zhang, Heyuan Jia, and Kaikai Wang), acquisition: (Heyuan Jia, Guocan Gu, Peng Zhang, Mingxin Zhang, Xuntao Yin and Yiying Mai, Yin), analysis: (Heyuan Jia, Kaikai Wang, Xia Wu and Congying Chu), interpretation: (Heyuan Jia, Kaikai Wang). All authors have been involved in the writing of the manuscript and approved the final version.

Declaration of interests

All authors declared they had no interests.

Acknowledgements

This study was supported by the STI2030-Major Projects 2021ZD0200201 and Beijing Municipal Public Welfare Development and Reform Pilot Project for Medical Research Institutes (grant ID: JYY202X-X).

Data Sharing Statement

The data collected for this study is not available to others.

References

1. Zhang P, Gu G, Duan Y, Zhuo Z, Pan C, Zuo P, et al. White matter alterations in pediatric brainstem glioma: An national brain tumor registry of China study. Front Neurosci. 2022;16:986873.
2. Boukaka RG, Beuriat PA, Di Rocco F, Vasiljevic A, Szathmari A, Mottolese C. Brainstem tumors in children: a monocentric series in the light of genetic and bio-molecular progress in pediatric neuro-oncology. Front Pediatr. 2023;11:1193474.
3. New PW, Thomas SJ. Cognitive impairments in the locked-in syndrome: A case report. Archives of Physical Medicine and Rehabilitation. 2005;86(2):338-43.
4. Omar R, Warren JD, Ron MA, Lees AJ, Rossor MN, Kartsounis LD. The neuro-behavioural syndrome of brainstem disease. Neurocase. 2007;13(5):452-65.
5. Aarsen FK, Van Dongen HR, Paquier PF, Van Mourik M, Catsman-Berrevoets CE. Long-term sequelae in children after cerebellar astrocytoma surgery. Neurology. 2004;62(8):1311-6.
6. Richter S, Schoch B, Ozimek A, Gorissen B, Hein-Kropp C, Kaiser O, et al. Incidence of dysarthria in children with cerebellar tumors: a prospective study. Brain Lang. 2005;92(2):153-67.
7. Baillieux H, De Smet HJ, Lesage G, Paquier P, De Deyn PP, Marien P. Neurobehavioral alterations in an adolescent following posterior fossa tumor resection. Cerebellum. 2006;5(4):289-95.
8. Kingma A, Mooij JJ, Metzemaekers JD, Leeuw JA. Transient mutism and speech disorders after posterior fossa surgery in children with brain tumours. Acta Neurochir (Wien). 1994;131(1-2):74-9.
9. LeBaron S, Zeltzer PM, Zeltzer LK, Scott SE, Marlin AE. Assessment of quality of survival in children with medulloblastoma and cerebellar astrocytoma. Cancer. 1988;62(6):1215-22.
10. Kupeli S, Yalcin B, Bilginer B, Akalan N, Haksal P, Buyukpamukcu M. Posterior fossa syndrome after posterior fossa surgery in children with brain tumors. Pediatr Blood Cancer. 2011;56(2):206-10.
11. Riva D, Giorgi C. The cerebellum contributes to higher functions during development: evidence from a series of children surgically treated for posterior fossa tumours. Brain. 2000;123 (Pt 5):1051-61.
12. Kirk EA, Howard VC, Scott CA. Description of posterior fossa syndrome in children after posterior fossa brain tumor surgery. J Pediatr Oncol Nurs. 1995;12(4):181-7.
13. Wolfe-Christensen C, Mullins LL, Scott JG, McNall-Knapp RY. Persistent psychosocial problems in children who develop posterior fossa syndrome after medulloblastoma resection. Pediatr Blood Cancer. 2007;49(5):723-6.
14. Jia HY, Zhang P, Gu GC, Li T, Jiang Z, Wu Z, et al. Brainstem tumors may increase the impairment of behavioral emotional cognition in children. J Neuro-Oncol. 2022;160(2):423-32.
15. Hansen JY, Cauzzo S, Singh K, Garcia-Gomar MG, Shine JM, Bianciardi M, et al. Integrating brainstem and cortical functional architectures. bioRxiv. 2023.
16. D'Aes T, Marien P. Cognitive and affective disturbances following focal brainstem lesions: a review and report of three cases. Cerebellum. 2015;14(3):317-40.

17. Zhang S, Ai L, Chen XZ, Wang K. Radiological Evaluation of Infratentorial Gangliogliomas in Various Anatomic Locations of the Cerebellum and Brainstem. Clin Neuroradiol. 2017;27(3):319-27.
18. Wei Y, Wang CH, Liu JC, Miao PF, Wu LB, Wang YY, et al. Longitudinal gray matter atrophy and accompanied functional connectivity alterations in patients with pontine infarction. Neurological Research. 2022;44(8):667-76.
19. Mah S, deVeber G, Wei XC, Liapounova N, Kirton A. Cerebellar Atrophy in Childhood Arterial Ischemic Stroke Acute Diffusion MRI Biomarkers. Stroke. 2013;44(9):2468-74.
20. Hartmann-von Monakow K, Akert K, Kunzle H. Projection of precentral, premotor and prefrontal cortex to the basilar pontine grey and to nucleus reticularis tegmenti pontis in the monkey (Macaca fascicularis). Schweiz Arch Neurol Neurochir Psychiatr. 1981;129(2):189-208.
21. Schmahmann JD, Ko R, MacMore J. The human basis pontis: motor syndromes and topographic organization. Brain. 2004;127(Pt 6):1269-91.
22. Brodal P. The corticopontine projection in the rhesus monkey. Origin and principles of organization. Brain. 1978;101(2):251-83.
23. Schmahmann JD, Pandya DN. Course of the fiber pathways to pons from parasensory association areas in the rhesus monkey. J Comp Neurol. 1992;326(2):159-79.
24. Zhang ZY, Liu ZQ, Qin W, Chen YW, Liu ZJ. Clinical and Radiological Features of Wallerian Degeneration of the Middle Cerebellar Peduncles Secondary to Pontine Infarction. Chinese Med J-Peking. 2018;131(6):665-+.
25. Zhang J, Meng L, Qin W, Liu N, Shi FD, Yu C. Structural damage and functional reorganization in ipsilesional m1 in well-recovered patients with subcortical stroke. Stroke. 2014;45(3):788-93.
26. Jang SH. Motor outcome and motor recovery mechanisms in pontine infarct: a review. NeuroRehabilitation. 2012;30(2):147-52.
27. Schmahmann JD, Pandya DN. The Cerebrocerebellar System. International Review of Neurobiology1997. p. 31-60.
28. Snider RS, Maiti A. Cerebellar contributions to the Papez circuit. J Neurosci Res. 1976;2(2):133-46.
29. Stoodley CJ, Schmahmann JD. Evidence for topographic organization in the cerebellum of motor control versus cognitive and affective processing. Cortex. 2010;46(7):831-44.
30. Buckner RL, Krienen FM, Castellanos A, Diaz JC, Yeo BTT. The organization of the human cerebellum estimated by intrinsic functional connectivity. Journal of Neurophysiology. 2011;106(5):2322-45.
31. Guell X, Gabrieli JDE, Schmahmann JD. Triple representation of language, working memory, social and emotion processing in the cerebellum: convergent evidence from task and seed-based resting-state fMRI analyses in a single large cohort. Neuroimage. 2018;172:437-49.
32. Stoodley CJ, Valera EM, Schmahmann JD. Functional topography of the cerebellum for motor and cognitive tasks: an fMRI study. Neuroimage. 2012;59(2):1560-70.
33. Stoodley CJ, Schmahmann JD. Functional topography in the human cerebellum: A meta-analysis of neuroimaging studies. Neuroimage. 2009;44(2):489-501.

34. Bushara KO, Wheat JM, Khan A, Mock BJ, Turski PA, Sorenson J, et al. Multiple tactile maps in the human cerebellum. Neuroreport. 2001;12(11):2483-6.
35. Schmahmann JD, Sherman JC. Cerebellar cognitive affective syndrome. Int Rev Neurobiol. 1997;41:433-40.
36. Schmahmann JD, Weilburg JB, Sherman JC. The neuropsychiatry of the cerebellum - insights from the clinic. Cerebellum. 2007;6(3):254-67.
37. Riva D, Giorgi C. The cerebellum contributes to higher functions during development - Evidence from a series of children surgically treated for posterior fossa tumours. Brain. 2000;123:1051-4.
38. Xi-Nian Z, Consortium C. developing Chinese Color Nest Project (devCCNP) Lite. Science Data Bank; 2024.
39. Han S, Carass A, He Y, Prince JL. Automatic cerebellum anatomical parcellation using U-Net with locally constrained optimization. Neuroimage. 2020;218:116819.
40. Carass A, Cuzzocreo JL, Han S, Hernandez-Castillo CR, Rasser PE, Ganz M, et al. Comparing fully automated state-of-the-art cerebellum parcellation from magnetic resonance images. Neuroimage. 2018;183:150-72.
41. Tustison NJ, Avants BB, Cook PA, Zheng YJ, Egan A, Yushkevich PA, et al. N4ITK: Improved N3 Bias Correction. Ieee T Med Imaging. 2010;29(6):1310-20.
42. Fonov V, Evans AC, Botteron K, Almli CR, McKinstry RC, Collins DL, et al. Unbiased average age-appropriate atlases for pediatric studies. Neuroimage. 2011;54(1):313-27.
43. Yushkevich PA, Piven J, Hazlett HC, Smith RG, Ho S, Gee JC, et al. User-guided 3D active contour segmentation of anatomical structures: Significantly improved efficiency and reliability. Neuroimage. 2006;31(3):1116-28.
44. Neo WS, Suzuki T, Kelleher BL. Structural validity of the Child Behavior Checklist (CBCL) for preschoolers with neurogenetic syndromes. Res Dev Disabil. 2021;109:103834.
45. Johnson WE, Li C, Rabinovic A. Adjusting batch effects in microarray expression data using empirical Bayes methods. Biostatistics. 2007;8(1):118-27.
46. Fortin JP, Cullen N, Sheline YI, Taylor WD, Aselcioglu I, Cook PA, et al. Harmonization of cortical thickness measurements across scanners and sites. Neuroimage. 2018;167:104-20.
47. Fortin JP, Parker D, Tunç B, Watanabe T, Elliott MA, Ruparel K, et al. Harmonization of multi-site diffusion tensor imaging data. Neuroimage. 2017;161:149-70.
48. Marquand AF, Rezek I, Buitelaar J, Beckmann CF. Understanding Heterogeneity in Clinical Cohorts Using Normative Models: Beyond Case-Control Studies. Biol Psychiat. 2016;80(7):552-61.
49. Verdi S, Kia SM, Yong KXX, Tosun D, Schott JM, Marquand AF, et al. Revealing Individual Neuroanatomical Heterogeneity in Alzheimer Disease Using Neuroanatomical Normative Modeling. Neurology. 2023;100(24).
50. Cui ZX, Pines AR, Larsen B, Sydnor VJ, Li HM, Adebimpe A, et al. Linking Individual Differences in Personalized Functional Network Topography to Psychopathology in Youth. Biol Psychiat. 2022;92(12):973-83.
51. Lou X, Gui QP, Sun L, Wu NZ, Lyu JH, Ma L. Comparisons of MR Findings Between

Supratentorial and Infratentorial Gangliogliomas. Clin Neuroradiol. 2016;26(1):65-71.
52. Wei Y, Wang C, Liu J, Miao P, Wu L, Wang Y, et al. Longitudinal gray matter atrophy and accompanied functional connectivity alterations in patients with pontine infarction. Neurol Res. 2022;44(8):667-76.
53. Sathyanesan A, Zhou J, Scafidi J, Heck DH, Sillitoe RV, Gallo V. Emerging connections between cerebellar development, behaviour and complex brain disorders. Nature Reviews Neuroscience. 2019;20(5):298-313.
54. Pierson CR, Al Sufiani F. Preterm birth and cerebellar neuropathology. Seminars in Fetal and Neonatal Medicine. 2016;21(5):305-11.
55. Takahashi E, Hayashi E, Schmahmann JD, Ellen Grant P. Development of cerebellar connectivity in human fetal brains revealed by high angular resolution diffusion tractography. NeuroImage. 2014;96:326-33.
56. Re TJ, Levman J, Lim AR, Righini A, Grant PE, Takahashi E. High-angular resolution diffusion imaging tractography of cerebellar pathways from newborns to young adults. Brain and Behavior. 2017;7(1).
57. <Cerebellar atrophy after moderate-to-severe pediatric traumatic brain injury.pdf>.
58. Finnie JW, Van den Heuvel C, Gebski V, Manavis J, Summersides GE, Blumbergs PC. Effect of Impact on Different Regions of the Head of Lambs. Journal of Comparative Pathology. 2001;124(2-3):159-64.
59. Mah S, deVeber G, Wei XC, Liapounova N, Kirton A. Cerebellar atrophy in childhood arterial ischemic stroke: acute diffusion MRI biomarkers. Stroke. 2013;44(9):2468-74.
60. Van Overwalle F, Baetens K, Marien P, Vandekerckhove M. Social cognition and the cerebellum: A meta-analysis of over 350 fMRI studies. Neuroimage. 2014;86:554-72.
61. Olson IR, Hoffman LJ, Jobson KR, Popal HS, Wang Y. Little brain, little minds: The big role of the cerebellum in social development. Dev Cogn Neurosci. 2023;60:101238.
62. Chao OY, Zhang H, Pathak SS, Huston JP, Yang YM. Functional Convergence of Motor and Social Processes in Lobule IV/V of the Mouse Cerebellum. Cerebellum. 2021;20(6):836-52.
63. Limperopoulos C, Bassan H, Gauvreau K, Robertson RL, Sullivan NR, Benson CB, et al. Does Cerebellar Injury in Premature Infants Contribute to the High Prevalence of Long-term Cognitive, Learning, and Behavioral Disability in Survivors? Pediatrics. 2007;120(3):584-93.
64. Schmahmann JD, Guell X, Stoodley CJ, Halko MA. The Theory and Neuroscience of Cerebellar Cognition. Annual Review of Neuroscience, Vol 42. 2019;42:337-64.
65. Olson IR, Ploaker A, Ezzyat Y. The Enigmatic temporal pole: a review of findings on social and emotional processing. Brain. 2007;130:1718-31.
66. Carta I, Chen CH, Schott AL, Dorizan S, Khodakhah K. Cerebellar modulation of the reward circuitry and social behavior. Science. 2019;363(6424).
67. Pitsika M, Tsitouras V. Cerebellar mutism A review. J Neurosurg-Pediatr. 2013;12(6):604-14.
68. Ike KGO, de Boer SF, Buwalda B, Kas MJH. Social withdrawal: An initially adaptive behavior that becomes maladaptive when expressed excessively. Neurosci Biobehav Rev. 2020;116:251-67.
69. O'Connell LA, Hofmann HA. The Vertebrate mesolimbic reward system and social behavior

network: A comparative synthesis. The Journal of Comparative Neurology. 2011;519(18):3599-639.
70. Frazier MR, Hoffman LJ, Popal H, Sullivan-Toole H, Olino TM, Olson IR. A missing link in affect regulation: the cerebellum. Soc Cogn Affect Neurosci. 2022;17(12):1068-81.
71. Brossard-Racine M, du Plessis AJ, Limperopoulos C. Developmental cerebellar cognitive affective syndrome in ex-preterm survivors following cerebellar injury. Cerebellum. 2015;14(2):151-64.
72. Brossard-Racine M, Limperopoulos C. Cerebellar injury in premature neonates: Imaging findings and relationship with outcome. Semin Perinatol. 2021;45(7).

Figure legends

Figure 1. The radiological characteristics of patients with brainstem tumors. (A-C) The 3D-T1 weighted MRI images from left to right, representing axial, coronal, and sagittal positions, respectively. Moving from top to bottom, the primary tumor is located in the medulla oblongata, pons, and midbrain. The red arrow highlights the tumor tissue, characterized by an uneven low signal.

Figure 2. Data Analysis Flowchart. (A) Patient and Multi-site Healthy Children enrolled. **(B)** Patients' behaviors were assessed in the neurosurgical clinic using the Child Behavior Checklist. **(C)** Structural MRI (T1) data acquisition and processing. Patients' brainstem was excluded before segmentation. **(D)** All participants' 28 cerebellar regions were obtained by Automatic Cerebellum Anatomical Parcellation using U-Net with Locally Constrained Optimization. **(E)** Normative trajectory in the GPR Model. In each model, a Gaussian model of the volume of each brain region was established with age and sex as covariates. **(F)** The Z-score profile of individual cerebellar regions' volume. **(J)** Pearson correlation matrix of cerebellar regions and behavioral problems. **(H)** The deviations of cerebellar volume predict behaviors. (I) Feature weight maps for 26 cerebellar regions.

Figure 3. Normative model and the analysis of deviations. (A) The normative model was estimated using GPR. For the volume of 26 cerebellar lobes, the normative models were estimated. In each model, the volume of cerebellar regions was the response variable, and age and gender were covariates. These four subplots respectively show the normative trajectory for male patients and controls, with red dots representing patients and blue dots representing controls. **(B)** The violin plots displays differences of positive and negative deviations in gender between patients and controls. **(C)** Stacking histograms of 26 cerebellar regions with positive and negative deviation rates in patients. The blue and red bars represent negative and positive deviation, respectively. **(D)** Illustration of extreme negative deviation of cerebellar

regions (deviation rate >0.2).

Figure 4. Behavior prediction models using individualized tOC. The tOC predicts individuals' behaviors of glioma patients, including social problem, withdrawn problem. Scatterplot of the relationship between tOC and the social problem **(A)**, withdrawn problem **(B)**. The tOC predicted unseen individuals' social problem **(C)** and withdrawn problem **(D)**. Data points represent the predicted scores of the independent test data using five-fold cross-validation. The p-value was derived from permutation testing.

Figure 5. Behavioral prediction model of individual deviation of cerebellar volume. The deviations in cerebellar volume predict major behaviors observed in glioma patients, including social problem **(A)** and withdrawn problem **(B)**. Each data point on the graph represents the predicted scores (y-axis) of participants in a model trained on independent data using five-fold cross-validation. In each scatter plot, the five colors represent participants of the five subsets, respectively. The prediction accuracy of behavior is mean correction r between five folds. The p-value predicted for each behavior is significant. They are feature weight maps for 26 brain regions. The gray bar graph indicates that the p-value of the weight of this feature is not significant **(C-D)**. It indicated reduced cerebellum volume in Right X, Right V, Right IV, Left IX, Left VIII, Left X, Left V and Right VIIB drove the prediction of social problem **(C)**. This revealed that reduced cerebellum volume in Left V, Right IV, Vermis VII, Left X, Left IV, Left IX, Vermis VI, Right X, Right VIIB, Vermis X, Right Crus I and Right V drove the prediction of withdrawn problem **(D)**.

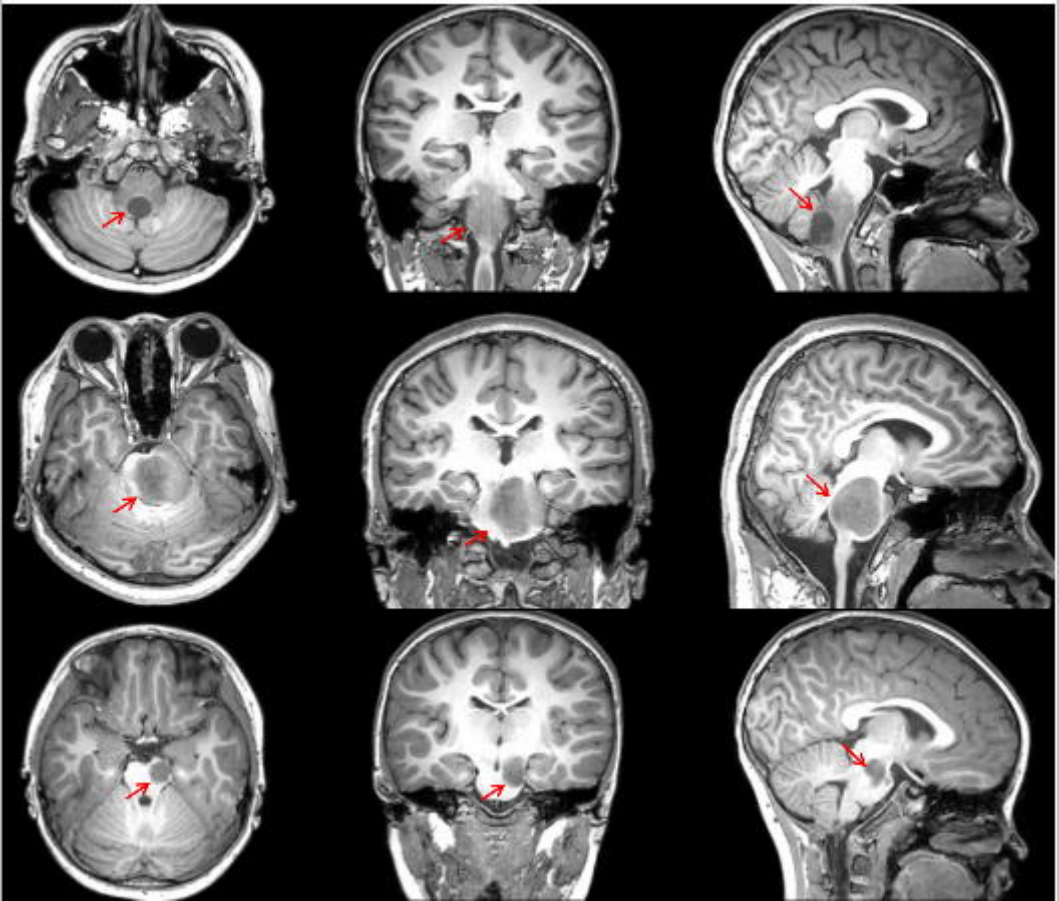

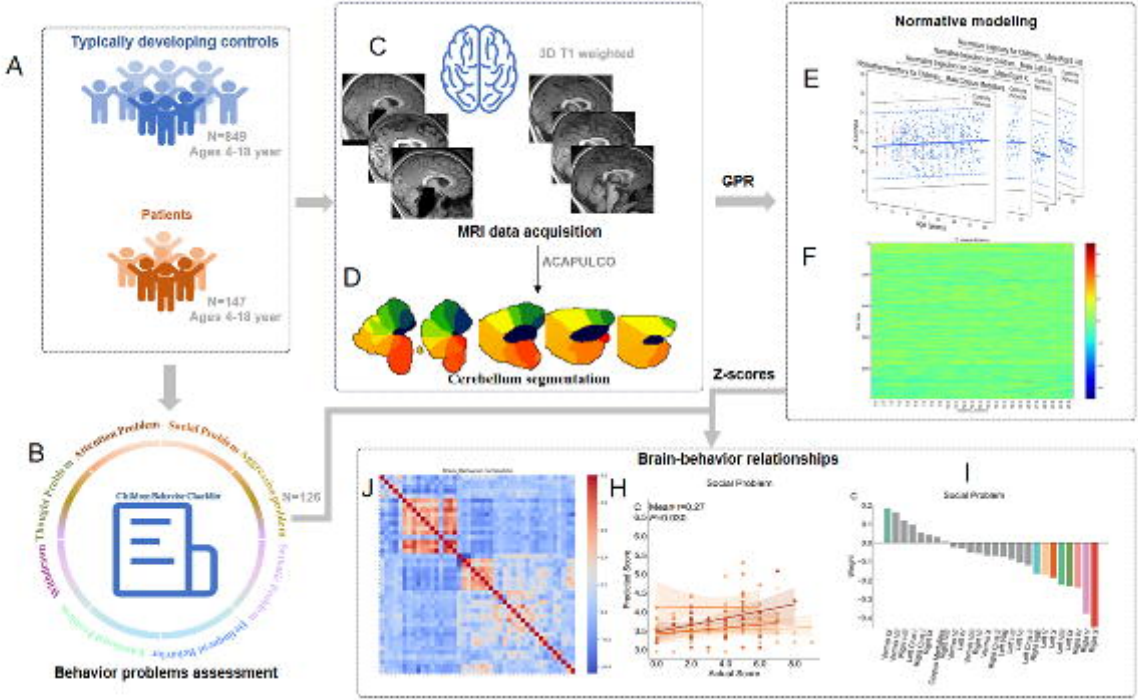
A
Typically developing controls
N=849
Ages 4-18 year
Patients
N=147
Ages 4-18 year
B
Behavior problems assessment
N=126
C
3D T1 weighted
MRI data acquisition
ACAPULCO
D
Cerebellum segmentation
GPR
Z-scores
Normative modeling
E
F
Brain-behavior relationships
J
H
Social Problem
I
Social Problem

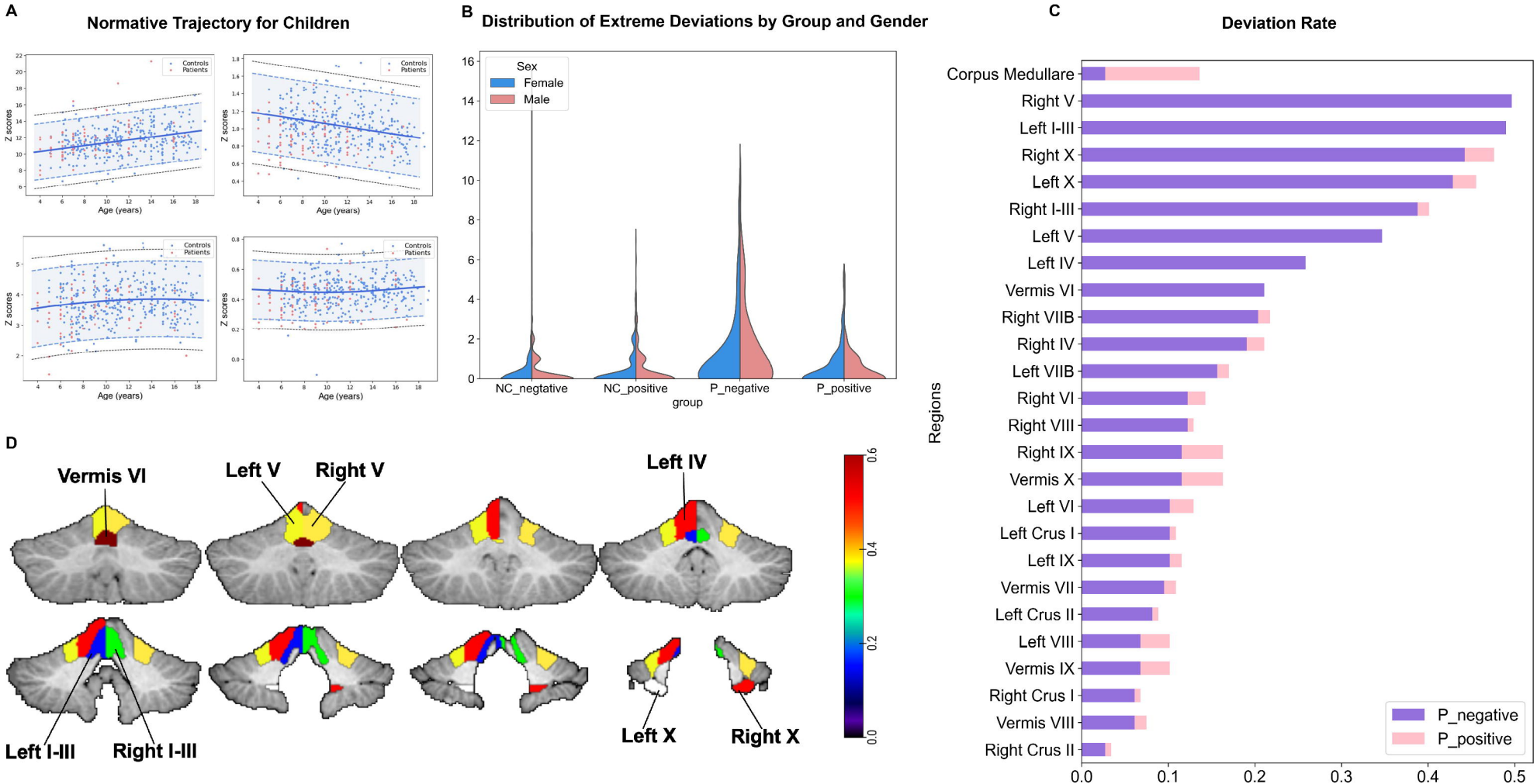
A
Normative Trajectory for Children
Controls
Patients
Z scores
Age (years)
B
Distribution of Extreme Deviations by Group and Gender
Sex
Female
Male
NC_negtative
NC_positive
P_negative
P_positive
group
C
Deviation Rate
Regions
Corpus Medullare
Right V
Left I-III
Right X
Left X
Right I-III
Left V
Left IV
Vermis VI
Right VIIB
Right IV
Left VIIB
Right VI
Right VIII
Right IX
Vermis X
Left VI
Left Crus I
Left IX
Vermis VII
Left Crus II
Left VIII
Vermis IX
Right Crus I
Vermis VIII
Right Crus II
P_negative
P_positive
D
Vermis VI
Left V
Right V
Left IV
Left I-III
Right I-III
Left X
Right X

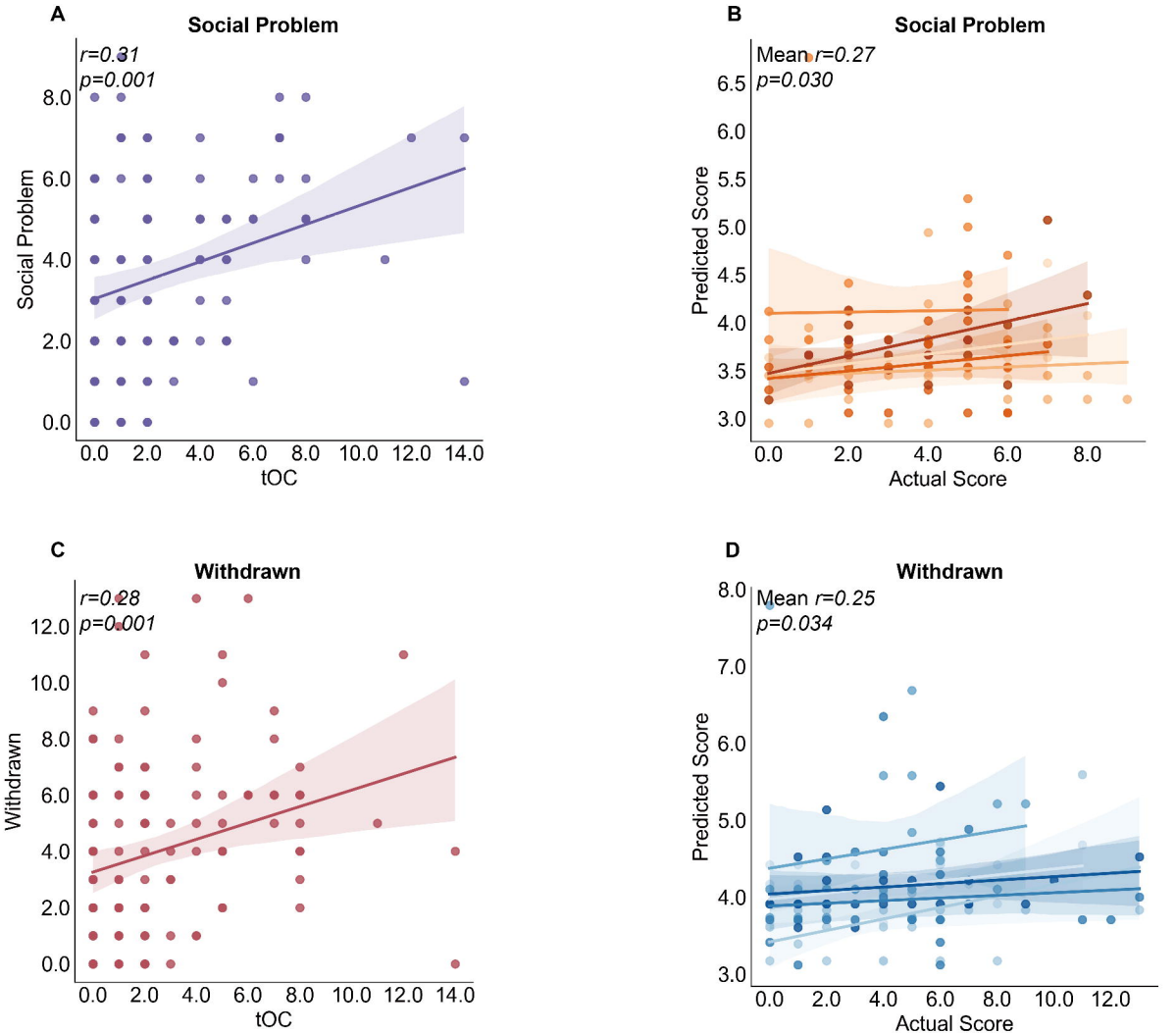
A
Social Problem
r=0.31
p=0.001
Social Problem
tOC
B
Social Problem
Mean r=0.27
p=0.030
Predicted Score
Actual Score
C
Withdrawn
r=0.28
p=0.001
Withdrawn
tOC
D
Withdrawn
Mean r=0.25
p=0.034
Predicted Score
Actual Score

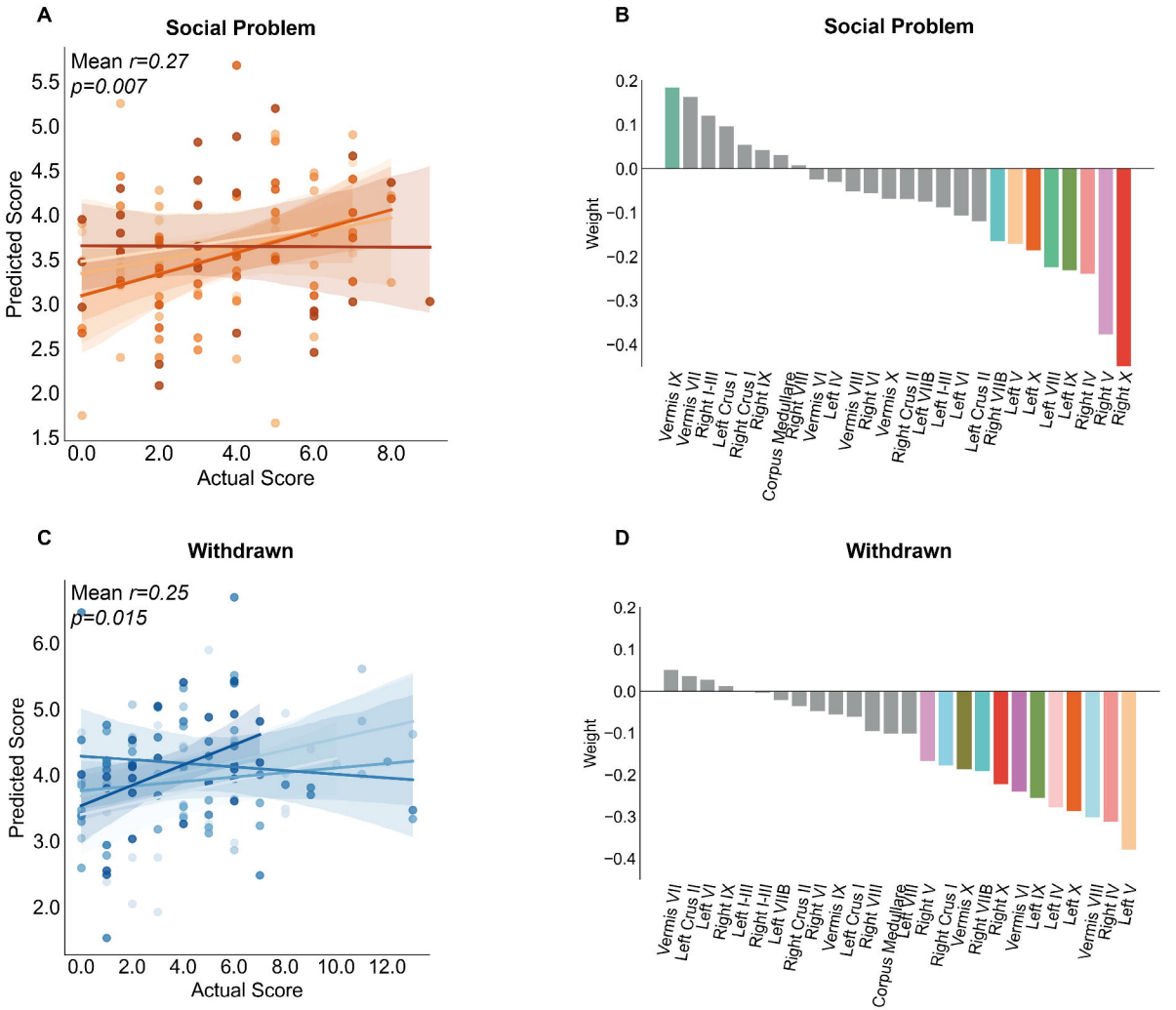
A
Social Problem
Mean r=0.27
p=0.007
Predicted Score
Actual Score
B
Social Problem
Weight
Vermis IX
Vermis VII
Right I-III
Left Crus I
Right Crus I
Right IX
Corpus Medullare
Right VIII
Vermis VI
Left IV
Vermis VIII
Right VI
Vermis X
Right Crus II
Left VIIB
Left I-III
Left VI
Left Crus II
Right VIIB
Left V
Left X
Left VIII
Left IX
Right IV
Right V
Right X
C
Withdrawn
Mean r=0.25
p=0.015
Predicted Score
Actual Score
D
Withdrawn
Weight
Vermis VII
Left Crus II
Left VI
Right IX
Left I-III
Right I-III
Left VIIB
Right Crus II
Right VI
Vermis IX
Left Crus I
Right VIII
Corpus Medullare
Left VIII
Right V
Right Crus I
Vermis X
Right VIIB
Right X
Vermis VI
Left IX
Left IV
Left X
Vermis VIII
Right IV
Left V